Marine Chemistry 245 (2022) 104150

Contents lists available at ScienceDirect

Marine Chemistry

journal homepage: www.elsevier.com/locate/marchem

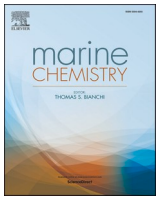

Gaining insights into the seawater carbonate system using discrete fCO_2 measurements

Maribel I. García-Ibáñez [a,b,*], Yui Takeshita [c], Elisa F. Guallart [d,b], Noelia M. Fajar [d,e], Denis Pierrot [f], Fiz F. Pérez [e], Wei-Jun Cai [g], Marta Álvarez [d]

[a] Centre for Ocean and Atmospheric Sciences, School of Environmental Sciences, University of East Anglia, Norwich, United Kingdom
[b] Institut de Ciències del Mar (ICM), CSIC, Barcelona 08003, Spain
[c] Monterey Bay Aquarium Research Institute, 7700 Sandholdt Road, Moss Landing, CA 95039, USA
[d] Instituto Español de Oceanografía (IEO), CSIC, A Coruña 15001, Spain
[e] Instituto de Investigaciones Marinas (IIM), CSIC, Vigo 36208, Spain
[f] Atlantic Oceanographic and Meteorological Laboratory (AOML), National Oceanic and Atmospheric Administration, 4301 Rickenbacker Causeway, Miami, FL 33149, USA
[g] School of Marine Science and Policy, University of Delaware, Newark, Delaware 19716, USA

ARTICLE INFO

Keywords:
Seawater
Dissolved inorganic carbon
Alkalinity
pH
Carbonate chemistry
Atlantic Ocean
Pacific Ocean
Southern Ocean
pCO_2
Seawater chemistry
Spectrophotometric pH

ABSTRACT

Understanding the ocean carbon sink and its future acidification-derived changes requires accurate and precise measurements with good spatiotemporal coverage. In addition, a deep knowledge of the thermodynamics of the seawater carbonate system is key to interconverting between measured and calculated variables. To gain insights into the remaining inconsistencies in the seawater carbonate system, we assess discrete water column measurements of carbon dioxide fugacity (fCO_2), dissolved inorganic carbon (DIC), total alkalinity (TA), and pH measured with unpurified indicators, from hydrographic cruises in the Atlantic, Pacific, and Southern Oceans included in GLODAPv2.2020 (19,013 samples). An agreement of better than ± 3% between fCO_2 measured and calculated from DIC and pH is obtained for 94% of the compiled dataset, while when considering fCO_2 measured and calculated from DIC and TA, the agreement is better than ± 4% for 88% of the compiled dataset, with a poorer internal consistency for high-CO_2 waters. Inspecting all likely sources of uncertainty from measured and calculated variables, we conclude that the seawater carbonate system community needs to (i) further refine the thermodynamic model of the seawater carbonate system, especially K_2, including the impact of organic compounds and other acid-base systems on TA; (ii) update the standard operating procedures for the seawater carbonate system measurements following current technological and analytical advances, paying particular attention to the pH methodology that is the one that evolved the most; (iii) encourage measuring discrete water column fCO_2 to further check the internal consistency of the seawater carbonate system, especially given the new era of sensor-based seawater measurements; and (iv) develop seawater Certified Reference Materials (CRMs) for fCO_2 and pH together with seawater CRMs for TA and DIC over the range of values encountered in the global ocean. Our conclusions also suggest the need for a re-evaluation of the adjustments applied by GLODAPv2 to pH, which were based on DIC and TA consistency checks but not supported by fCO_2 and DIC consistency.

1. Introduction

Since the industrial revolution, the global ocean has absorbed approximately 30% of anthropogenic carbon dioxide (CO_2) emissions (Gruber et al., 2019; Friedlingstein et al., 2022). The resulting increase in seawater CO_2 has caused an unprecedented, rapid, and long-term change in ocean chemistry, a process known as ocean acidification (e.g., Caldeira and Wickett, 2003; Raven et al., 2005; Gattuso et al., 2014; Williamson and Widdicombe, 2018). Monitoring such changes in the interior ocean and the air-sea CO_2 fluxes requires accurate and precise measurements with good spatiotemporal coverage. To that end, the seawater carbonate system community has devoted huge efforts to compile and quality control measurements of the seawater carbonate system to produce internally-consistent and quality-controlled products

* Corresponding author at: Institut de Ciències del Mar (ICM), CSIC, Barcelona 08003, Spain.
E-mail address: maribelgarcia@icm.csic.es (M.I. García-Ibáñez).

https://doi.org/10.1016/j.marchem.2022.104150
Received 24 December 2021; Received in revised form 14 July 2022; Accepted 19 July 2022
Available online 22 July 2022

that are easily usable, coherent, and readily available, such as SOCAT (Surface Ocean CO_2 Atlas) and GLODAP (Global Ocean Data Analysis Project). SOCAT compiles quality-controlled measurements of surface CO_2 fugacity (fCO_2) with wide spatiotemporal coverage (Bakker et al., 2016). GLODAP compiles water column measurements from trans-oceanic cruises of twelve core variables, including discrete water column measurements of dissolved inorganic carbon (DIC), total alkalinity (TA), pH, and, for the first time in GLODAPv2.2020, fCO_2 (Olsen et al., 2020). The relevance and utility of both data products are of utmost for stakeholders and the scientific community in evaluating and predicting the ocean carbon sink and consequences of global change (Guidi et al., 2020; Tanhua et al., 2021).

Surface and water column autonomous systems have been developed to improve the spatiotemporal coverage of ocean carbon monitoring, although pH and fCO_2 are the only seawater carbonate system variables routinely measured autonomously (Bushinsky et al., 2019). Great efforts have been invested in calibrating sensor-based pH with discrete fCO_2 and pH measurements and/or those derived from DIC and TA (Williams et al., 2017; Takeshita et al., 2018), requiring in-depth knowledge of the chemistry of the seawater carbonate system to consistently evaluate its variables and their interconversion.

Despite the efforts of the community to improve our understanding of the seawater carbonate system, significant inconsistencies remain when comparing measured and calculated variables. Among the sources of the remaining inconsistencies are the discrepancy between measured pH and pH calculated from TA and DIC, the debated existence and magnitude of organic alkalinity (OrgAlk), and the parameterization of the dissociation constants (e.g., McElligott et al., 1998; Fong and Dickson, 2019; Raimondi et al., 2019; Álvarez et al., 2020; Kerr et al., 2021; Takeshita et al., 2021; Woosley, 2021). A poor intercomparability between measured and calculated seawater carbonate system variables could generate a lack of temporal coherence for estimates of ocean acidification, carbon storage, and air-sea CO_2 fluxes derived from non-comparable measurements and/or improperly adjusted sensor data. For example, a 1.3 μatm systematic bias in fCO_2 leads to a 0.2 Pg C yr^{-1} bias in the global integrated air-sea CO_2 flux (Wanninkhof et al., 2013a), representing about 7% of the total flux of 2.8 ± 0.4 Pg C yr^{-1} for 2011–2020 (Friedlingstein et al., 2022).

In this work, we exploit the availability of discrete water column measurements of fCO_2 in GLODAPv2.2020 to gain new insights into the causes of the remaining inconsistencies in the seawater carbonate system. Measurements of fCO_2 can be used to evaluate the internal consistency of the seawater carbonate system when the system is overdetermined, i.e., studying the agreement between measured and calculated variables when concomitant measurements of at least two of the three other main carbonate system variables (DIC, TA, and pH) are performed in a seawater sample. The uncertainty of the calculated values depends on the uncertainty of the input variables and the thermodynamic constants, and the correct accounting for all relevant acid-base systems. Using the combination of variables pH, fCO_2, and DIC for internal consistency exercises does not rely on assumptions about OrgAlk or the total boron to salinity ratio (r_B). Therefore, pH calculated from fCO_2 and DIC, and fCO_2 calculated from pH and DIC have uncertainties similar to directly measured values, generating lower uncertainty than when pH or fCO_2 are calculated with the input pair DIC-TA, where other acid-base systems affecting TA come into play (e.g., Park, 1969; Millero, 2007; Raimondi et al., 2019).

This work builds on that of McElligott et al. (1998), who evaluated the precision and thermodynamic consistency of discrete fCO_2 measurements using a database of ~2,500 samples with paired measurements of DIC, TA, pH, and fCO_2 from the Equatorial Pacific, where fCO_2 ranged from about 200 to 2,000 μatm. In the present work, we use a quality-controlled database of over 19,000 samples from the Atlantic, Pacific, and Southern Oceans, with fCO_2 ranging from 189 to 2,806 μatm. Since McElligott et al. (1998), the seawater carbonate system community has created and adopted standard operating procedures (SOPs) for measurements of DIC, TA, pH, and fCO_2 (Dickson et al., 2007) and uses Certified Reference Materials (CRMs) for TA and DIC (Dickson, 2010). Therefore, an updated evaluation of the thermodynamic consistency of discrete fCO_2 measurements should highlight the improvements the seawater carbonate system community has made and shed light on the remaining questions in the seawater carbonate system to be solved.

2. Materials and methods

2.1. Seawater carbonate system and ancillary data

We selected discrete water column measurements of fCO_2, DIC, and TA from GLODAPv2.2020 (Olsen et al., 2020) with the first quality control flag equal to 2 (World Ocean Circulation Experiment, WOCE, flag "acceptable"). A total of 19,013 samples from 16 cruises (Fig. 1 and Table S1) were selected. Spectrophotometric pH measurements on the total scale at 25 °C (hereafter pH) with a quality flag of 2 were also performed in 9 of the 16 cruises (11,633 samples; Table S1). Other ancillary data such as the inorganic nutrients (phosphate and silicic acid) were also extracted from GLODAPv2.2020. Missing values from phosphate and silicic acid were estimated with CANYON-B (Bittig et al., 2018), using as predicting parameters latitude, longitude, temperature, salinity, and, if possible, oxygen with a first quality control flag equal to 2. Interpolated inorganic nutrient from CANYON-B allowed us to recover 20% of the samples and generated fCO_2 values with a discrepancy lower than 0.2%. GLODAPv2.2021 did not contain additional cruises with discrete water column fCO_2 measurements (Lauvset et al., 2021).

The pH measurements were performed spectrophotometrically (Clayton and Byrne, 1993) with unpurified indicators from different manufacturers (Table S1). DIC samples were analyzed by coulometric titration and TA measurements were made by potentiometric titration (Dickson et al., 2007). All the selected cruises used CRMs as secondary standards for DIC and TA (Table S1), i.e., CRMs were utilized to account for instrument drift and maintain measurement accuracy (Dickson, 2010). Two types of instruments were used to measure discrete fCO_2 samples (Table S1). In both cases, an aliquot of seawater was equilibrated at a constant temperature (usually 20 °C; Table S1) with a headspace of known initial CO_2 content. Subsequently, the headspace CO_2 concentration was determined with a non-dispersive infrared analyzer (NDIR; Wanninkhof and Thoning, 1993) or by converting the CO_2 to CH_4 and then analyzing the concentration using a gas chromatograph with flame-ionization detection (GC-FID; Neill et al., 1997). A general precision of ± 0.5 μatm and an accuracy of 2 μatm are

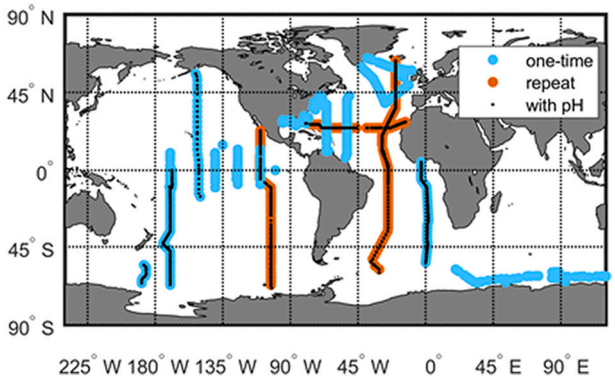

Fig. 1. Cruises available in GLODAPv2.2020 with discrete water column measurements of fCO_2, DIC, and TA. Orange circles indicate repeated cruise tracks, blue circles indicate one-time cruises, and black dots indicate cruises with measurements of all four variables: fCO_2, DIC, TA, and pH. (For interpretation of the references to color in this figure legend, the reader is referred to the web version of this article.)

commonly expected for fCO_2 measurements (Wanninkhof and Thoning, 1993), although the measurement precision varies with the fCO_2 content of the sample, being within 0.2–1% of the measured value (Chen et al., 1995; Neill et al., 1997).

GLODAPv2.2020 contained, for the first time, discrete water column fCO_2 measurements commonly reported at 20 °C (fCO_2 hereafter), which have been assigned quality flags (first quality control) but have not been secondary quality controlled (Olsen et al., 2020). GLODAP secondary quality control is performed on DIC, TA, and pH data using crossover analyses between overlapping cruises in deep waters, where minimum temporal changes are expected (Sabine et al., 2005). The secondary quality control aims to identify and correct any significant biases in the data while retaining any signal due to temporal changes. In the case of pH, due to the scarcity of measurements compared to DIC and TA, a combination of crossover and internal consistency analysis using pH, TA, and DIC were applied in GLODAPv2.2019 and previous versions (Olsen et al., 2019). GLODAPv2.2020 acknowledged that secondary quality control of the pH data using internal consistency might generate false corrections, so only crossover analysis was performed on the new cruises added to GLODAPv2.2020 (Olsen et al., 2020). However, the pH adjustments based on internal consistency applied in versions before GLODAPv2.2020 were not removed. Table S1 summarizes any adjustment applied to the seawater carbonate system variables by GLODAP. We emphasize that all the selected cruises have been secondary quality controlled for TA, DIC, and pH, a process aiming to produce a consistency better than ± 4 μmol kg^{-1} for DIC and TA and ± 0.01 for pH (Olsen et al., 2020).

2.2. Thermodynamic calculations and sensitivities

Our results on the internal consistency of the seawater carbonate system are presented as residuals or differences between the measured and the calculated variable from paired carbonate system measurements (Δ, measured minus calculated variable). All calculations were performed using the MATLAB® version of CO2SYSv3 (Sharp et al., 2020), with the carbonic acid dissociation constants (pK_1 and pK_2) of Mehrbach et al. (1973) reformulated on the total hydrogen scale by Lueker et al. (2000), the bisulfate dissociation constant of Dickson (1990), and the r_B ratio of Lee et al. (2010). The CO2SYSv3 was modified to include the recent pK_2 from Schockman and Byrne (2021) combined with pK_1 from Waters et al. (2014).

Input variables were perturbed by up to five times the total estimated standard uncertainty for the variables and the thermodynamic constants following the procedure of Álvarez et al. (2020) to assess the influence of input parameter uncertainties in the calculated values. The estimated standard uncertainty for the variables and the thermodynamic constants used were ± 4 μmol kg^{-1} for TA and DIC, ± 0.01 for pH, ± 1% for fCO_2, ± 0.0075 for pK_1, ± 0.015 for pK_2, ± 0.01 for the borate constant (pK_B), and ± 2% for r_B (Neill et al., 1997; Wanninkhof et al., 2003; Orr et al., 2018; Olsen et al., 2020).

Ocean fCO_2 and hydrogen ion concentration (10^{-pH}) are almost linearly related when both variables are expressed on a logarithmic scale, as both variables are pressure- and temperature-dependent (Fig. S1). This fact translates into an almost linear effect (in %) of pH uncertainties on fCO_2 calculated from pH and DIC (fCO_2(pH,DIC)) that are inversely correlated across the seawater pH range. Uncertainties in fCO_2(pH,DIC) are mostly dependent on uncertainties in pH and pK_1 (Fig. S2). Uncertainties in pK_2 play a minor role in fCO_2(pH,DIC) and are significant only for high-pH waters (pH > 7.8), and they are about an order of magnitude lower than that of pK_1 (Fig. S2D). Uncertainties in DIC play a minor role in generating uncertainties in fCO_2(pH,DIC) (Fig. S2B).

Calculated fCO_2 from TA and DIC (fCO_2(TA,DIC)) is more uncertain than fCO_2(pH,DIC) because of the interplay of additional uncertainties in r_B and pK_B (Fig. S3) and any presence of OrgAlk, which is not included in the inorganic carbonate system acid-base model and is usually evaluated as inconsistencies between calculated and measured TA (Kerr et al., 2021). Unlike fCO_2(pH,DIC), uncertainties in pK_2 play a major role for fCO_2(TA,DIC) and are of similar magnitude to the uncertainties in pK_1. Besides, fCO_2(TA,DIC) is highly sensitive to relatively small uncertainties in DIC and TA. For high-pH waters (pH > 7.8), uncertainties in r_B and pK_B also contribute to uncertainties in fCO_2(TA,DIC) (Fig. S3).

The combined propagated standard uncertainty in calculated fCO_2 and other seawater carbonate system variables was estimated using the *errors* routine from Orr et al. (2018), using the total estimated standard uncertainties for the thermodynamic constants and variables listed above. Considering the uncertainty of 0.01 in pH and 4 μmol kg^{-1} in DIC, the uncertainty in fCO_2(pH,DIC) is about 2.5%, slightly increasing with pH (yellow stars in Fig. 2). The uncertainty in fCO_2(pH,DIC) increases to about 3% when adding the uncertainty in the thermodynamic constants (orange stars in Fig. 2). An uncertainty of 4 μmol kg^{-1} in DIC and TA generates a combined standard uncertainty in fCO_2(TA,DIC) of about 2% for high-pH waters (with pH > 8) and about 4% for low-pH waters (pH < 7.6) (light-blue stars in Fig. 2). Including the uncertainty in the thermodynamic constants, the combined standard uncertainty in fCO_2(TA,DIC) increases to about 4.5% over the entire pH range (navy stars in Fig. 2). Including the uncertainty of 1% in measured fCO_2, the resulting combined standard uncertainty in ΔfCO_2(TA,DIC) and ΔfCO_2(pH,DIC) is about ± 4.5% and ± 3%, respectively, with small variations over the oceanic pH range (black lines in Figs. 2 and 3). Combined standard uncertainties in the residuals from the other seawater carbonate system variables (TA, pH, and DIC using different input pairs) are calculated accordingly, considering the uncertainties of the input pair, thermodynamic constants and the measured variable.

We want to highlight that our internal consistency assessment is based on measurements under a specific temperature and at atmospheric pressure. However, different outcomes may result when evaluating the variables at in situ temperature and pressure conditions (Ribas-Ribas et al., 2014; Raimondi et al., 2019; Sulpis et al., 2020).

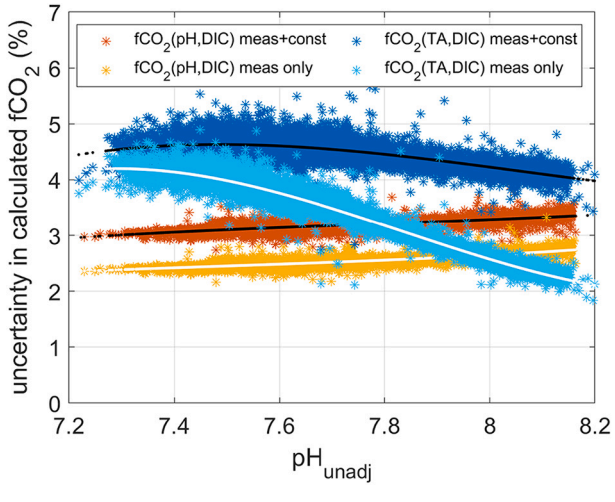

Fig. 2. Standard uncertainty in calculated fCO_2 (in %) introduced by the input variables and thermodynamic constants versus pH (original unadjusted pH, pH_{unadj}). Results derived from the *errors* routine from Orr et al. (2018) using imposed uncertainties in the measurements from GLODAP and zero or default uncertainties in the thermodynamic constants. Ascribed measurement uncertainties from GLODAP: ± 0.01 for pH and ± 4 μmol kg^{-1} for DIC and TA. Default uncertainties in the dissociation constants: ± 0.002 for pK_0, ± 0.0075 for pK_1, ± 0.015 for pK_2, ± 0.01 for pK_B, and ± 0.01 for pK_w (water). (For interpretation of the references to color in this figure legend, the reader is referred to the web version of this article.)

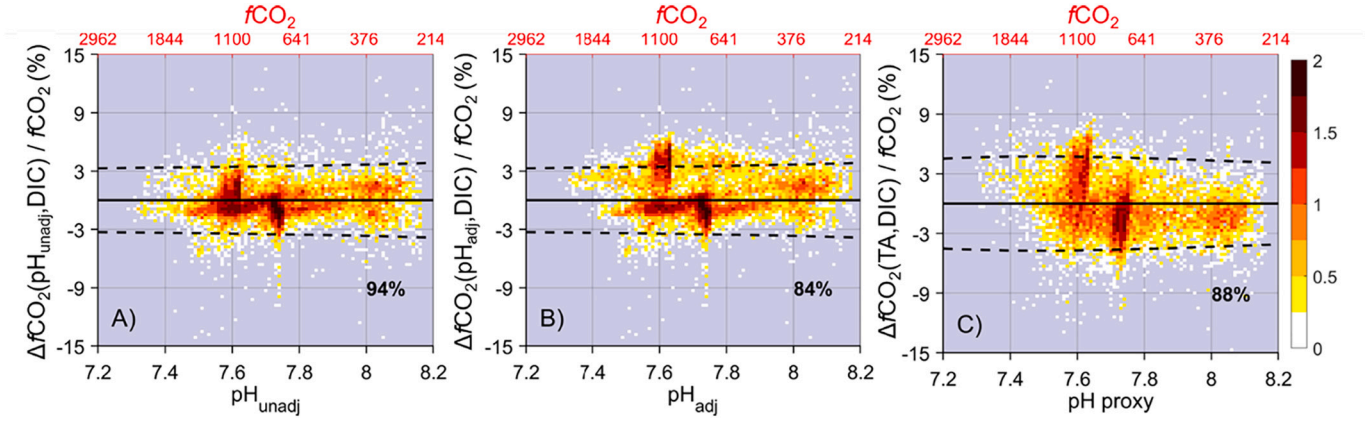

Fig. 3. Two-dimensional histograms showing the logarithm of the number of observations (z-axis in color scale) of $\Delta fCO_2/fCO_2$ (measured minus calculated fCO_2 divided by measured fCO_2, all at 20 °C; in %; y-axes) versus pH (on the total scale at 25 °C; bottom x-axes) and fCO_2 (at 20 °C; in µatm; top x-axes; note the reverse axes) from (A-B) fCO_2(pH,DIC) and (C) fCO_2(TA,DIC). The bin-width used to count the data is 0.01 pH units on the x-axes and 0.3% on the y-axes. Subplot A shows the results using unadjusted original pH data, while subplot B shows the results using GLODAP-adjusted pH data. In subplot C, the pH depicted in the bottom x-axis is a reconstruction of pH based on DIC and TA (pH proxy). Dashed lines depict the combined standard uncertainty in calculated fCO_2 resulting from the propagation of uncertainties in the input variables and thermodynamic constants and the uncertainty of the measured variable (i.e., fCO_2). The percentages indicate the number of samples within the combined standard uncertainty limits (dashed lines). Calculations were performed at sample salinity and atmospheric pressure.

3. Results and discussion

3.1. Distribution and magnitude of fCO_2 residuals (ΔfCO_2, measured minus calculated) and overall consistency

Theoretically, the combined standard uncertainty from measured seawater carbonate system variables and thermodynamic constants precludes estimating fCO_2 from other seawater carbonate system variables with an uncertainty lower than that needed to fulfil the GOA-ON climate-quality goal (± 0.5% standard uncertainty) or even the weather-quality goal (± 2.5% standard uncertainty) (Newton et al., 2015) (Fig. 2). However, our results show that 94% of ΔfCO_2(pH,DIC) and 88% of ΔfCO_2(TA,DIC) are comprised within the expected combined standard uncertainty limits (Fig. 3 dashed lines). Particularly, the distribution of ΔfCO_2(pH,DIC) using original unadjusted pH (fCO_2(-pH_{unadj},DIC)) centers around zero (ΔfCO_2(pH,DIC) = −0.3 ± 2%; mean and standard deviation), which points to measured fCO_2 being internally consistent with measured pH_{unadj} and DIC, although a slight ΔfCO_2 pH-dependency appears (Fig. 3A). Surprisingly, ΔfCO_2 split into two groups when fCO_2 is calculated using GLODAP-adjusted pH (fCO_2(pH_{adj},DIC)) (Figs. 3B, and S4). The adjustment of pH values in GLODAP (Table S1) translates into a constant bias (in %) in calculated fCO_2 (Fig. S2A). Note that GLODAPv2.2020 nor GLODAPv2.2021 did not study the internal consistency of the seawater carbonate system using fCO_2 data, so these inconsistencies with fCO_2 were undetected. For waters with pH < 7.8 (fCO_2 > ~650 µatm), mainly located below 500 m depth, measurements are less internally consistent, and the effect of pH adjustments based on the internal consistency of pH, DIC, and TA exacerbates the inconsistency between pH, DIC, and fCO_2 (Fig. 3A and B), changing the mean ΔfCO_2(pH,DIC) from −0.3 ± 2% (using the original unadjusted pH) to 0.5 ± 2.5% (using pH adjusted by GLODAP). The better internal consistency of fCO_2(pH_{unadj},DIC) suggests the adjustments applied to original pH data by GLODAP should be re-evaluated. Consequently, the remaining discussion is based on unadjusted pH values (pH_{unadj}).

The distribution of ΔfCO_2(TA,DIC) (Fig. 3C) is slightly biased towards negative values and presents higher dispersion (−0.8 ± 7.1%; mean and standard deviation) than ΔfCO_2(pH,DIC) (−0.3 ± 2%). The wider dispersion of ΔfCO_2(TA,DIC) is related to the high sensitivity of fCO_2(TA,DIC) to relatively small uncertainties in DIC and TA, especially for high-fCO_2 (low-pH) waters, which adds to the effect of uncertainties in the thermodynamic constants (Fig. 2 and S3) and the difficulty in measuring high-fCO_2 waters. An uncertainty about 4 µmol kg^{-1} in DIC and TA generates a combined standard uncertainty in calculated fCO_2(TA,DIC) of about 2% for high-pH waters (with pH > 7.8; fCO_2 < ~650 µatm) and of about 4% for low-pH waters (pH < 7.8; fCO_2 > ~650 µatm) (light-blue stars in Fig. 2). If the uncertainty in the thermodynamic constants is also included, the combined standard uncertainty in calculated fCO_2(TA,DIC) increases to about 4.5% for the entire pH range (navy stars in Fig. 2). Accordingly, ΔfCO_2(TA,DIC) values for waters with pH > 7.8 (fCO_2 < ~650 µatm), mainly located in the upper 500 m of the ocean, distribute around −1.1 ± 2.4%, while those with pH < 7.8 distribute around −0.1 ± 3% (Fig. 3).

Patterns in Fig. 4 demonstrate the following facts regarding the overall internal consistency in the seawater carbonate system of the compiled dataset: (i) 83–87% of the samples are comprised within the limits of the combined standard uncertainty, and about 40% of the samples are comprised within half the value of the combined standard uncertainty (white rectangles in Fig. 4); and (ii) no clear groups of data are discerned that could point to biases in the measurements. Systematic biases in cruises and/or seawater carbonate system variables could be identified using plots like those in Fig. 4. For example, the GLODAP pH adjustments create a displacement in ΔfCO_2(pH_{adj},DIC) (Fig. S5A), and two groups of data in ΔpH_{adj}, ΔDIC, and ΔTA (Fig. S5 B and D), where the inconsistent data is far from the origin point (i.e., zero).

Comparing our results for ΔTA (Fig. 4C) with those in Fig. 5 in McElligott et al. (1998), we can see how the accuracy and precision of the TA and DIC measurements have improved by one order of magnitude as about 47% of the ΔTA (and also ΔDIC) values are centered in zero and < 0.2%; while in McElligott et al. (1998) residuals were < 2%. This fact is probably related to the general use of CRMs for DIC and TA (Dickson, 2010) and the availability of well-established SOPs (Dickson et al., 2007). Probably, the accuracy and precision of pH and fCO_2 measurements have also improved since the work of McElligott et al. (1998) but we cannot assess it as the pH data from the cruises used by McElligott et al. (1998) was disregarded in GLODAPv2.2020, and fCO_2 data was only maintained for one cruise in GLODAPv2.2020.

In the following sections, we assess the possible factors required to improve the internal consistency of the seawater carbonate system variables: the measurements of fCO_2, pH, DIC, and TA, and the thermodynamic constants.

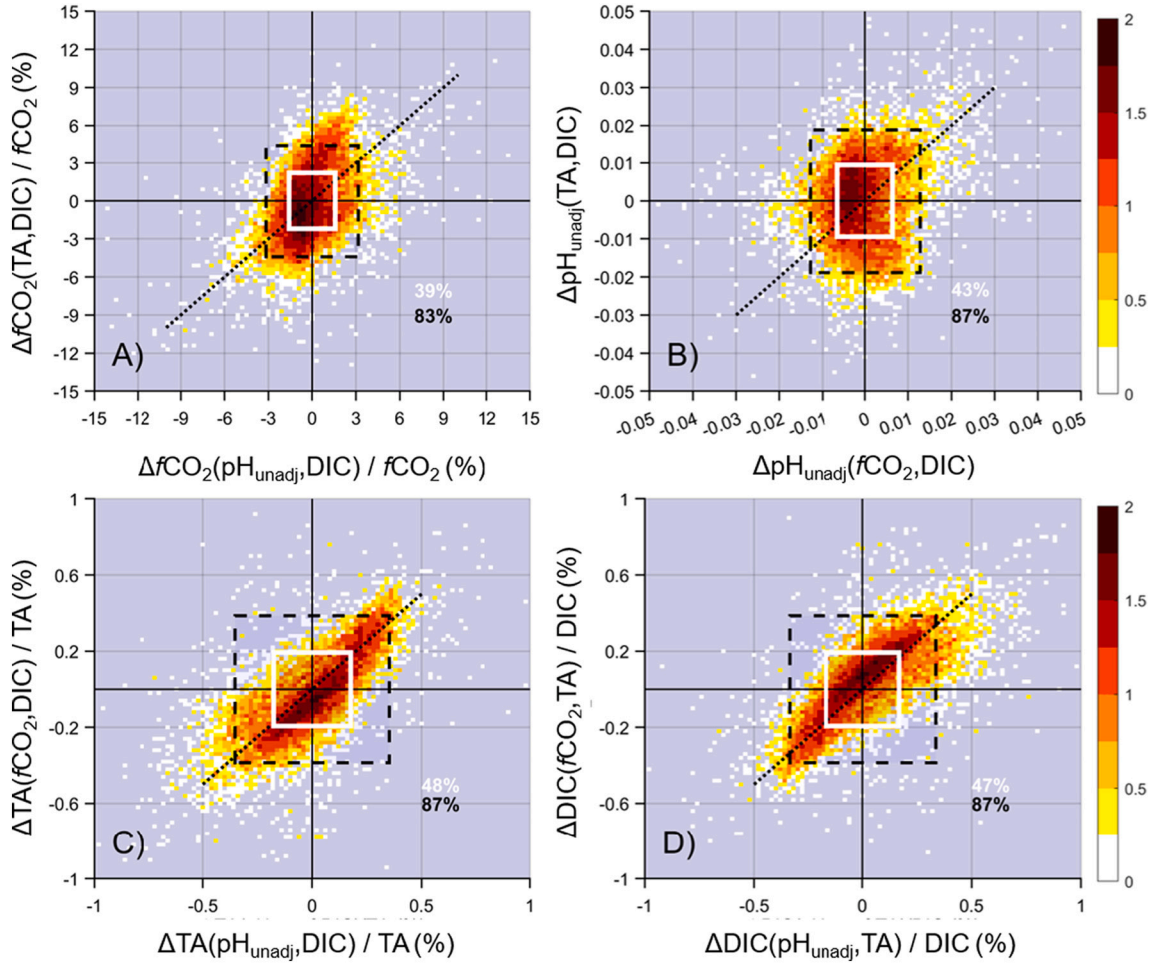

Fig. 4. Two-dimensional histograms showing the logarithm of the number of observations (z-axes in color scale) of (A) ΔfCO_2(TA,DIC)/fCO_2 versus ΔfCO_2(pH_{unadj}, DIC)/fCO_2 (both in %); (B) ΔpH_{unadj}(TA,DIC) versus ΔpH_{unadj}(fCO_2,DIC) (both in pH units); (C) $\Delta TA(fCO_2,DIC)/TA$ versus $\Delta TA(pH_{unadj},DIC)/TA$ (both in %); and (D) $\Delta DIC(fCO_2,TA)/DIC$ versus $\Delta DIC(pH_{unadj},TA)/DIC$ (both in %). Δs represent measured minus calculated variables. Unadjusted original pH values were used, and calculations were performed at sample salinity and atmospheric pressure. We refer the reader to Fig. S5 for results using pH_{adj}. Dotted diagonal lines are the 1:1 relationship, and black dashed-delimited squares are the combined standard uncertainty in calculated variables resulting from the propagation of uncertainties in the input variables and thermodynamic constants, as well as the uncertainty of the measured variable. The percentage values in black indicate the number of samples contained within the limits of the combined standard uncertainty. Lines and percentage values in white correspond to half the combined standard uncertainty.

3.2. Influence of the seawater carbonate system measurements fCO_2 measurements

The analytical and calibration particularities of the methodology to measure discrete fCO_2 in seawater are likely contributors to ΔfCO_2 outside the limits of the combined standard uncertainty in calculated fCO_2 (Fig. 3). As we will discuss below, they would not explain the slight pH-dependency of ΔfCO_2(pH,DIC) (Fig. 3A), the abundance of positive ΔfCO_2(TA,DIC) at low-pH values (Fig. 3C), or the high density of negative ΔfCO_2 (Fig. 4), which causes will be discussed in the following sections. However, the lack of CRMs for discrete fCO_2 measurements hampers the independent assessment of the accuracy of fCO_2 measurement, which is usually assessed using internal consistency checks (Wanninkhof et al., 2013c), inherently conditioned by the accuracy and precision of the other seawater carbonate system variables and the selection and uncertainty of thermodynamic constants.

The similar distributions of ΔfCO_2(pH_{unadj},DIC) and ΔfCO_2(TA,DIC) resulting from fCO_2 measurements performed with either GC-FID or NDIR (Fig. S6) discard the different techniques as a major contributor to ΔfCO_2. Besides, the comparative study performed by Chen et al. (1995) showed good agreement between measurements obtained with the two types of instrumentations.

The negative ΔfCO_2 values (Fig. 3; recall, Δ, measured minus calculated variable), especially for high-fCO_2 samples, could be caused by an underestimation of measured fCO_2 resulting from (i) CO_2 outgassing during sample collection and/or measurement, and/or (ii) insufficient equilibration time, the latter being unlikely since the equilibration time was long enough to achieve full equilibration (Chen et al., 1995). If the outgassing occurred during sample collection and/or sample thermostatization to 20 °C, this CO_2 loss would be proportional to sample fCO_2 and the difference between in situ and laboratory temperature and atmospheric fCO_2 (~400 µatm). We discard sample outgassing as a major contributor to ΔfCO_2 since (i) there isn't a significant relationship between ΔfCO_2 and in situ temperature or the difference between sample fCO_2 and atmospheric fCO_2 (Fig. S7), and (ii) the loss of CO_2 during the measurement would involve a leak in the loop that would invalidate the result, being the measurement flagged as bad.

Positive ΔfCO_2 values could be caused by an overestimation of measured fCO_2 related to technical and/or calibration issues in the fCO_2 measurement procedure. Water samples for fCO_2 measurements are equilibrated with a gas phase of known CO_2 content before analysis. This equilibration perturbs the fCO_2 in the water sample, but it is minimized by choosing a headspace gas with fCO_2 close to that of the water sample. In our selected cruises, gas standards with different CO_2 mixing ratios were used to create the headspace with the minimum fCO_2 difference from the expected fCO_2 in the water sample. For the NDIR system, a

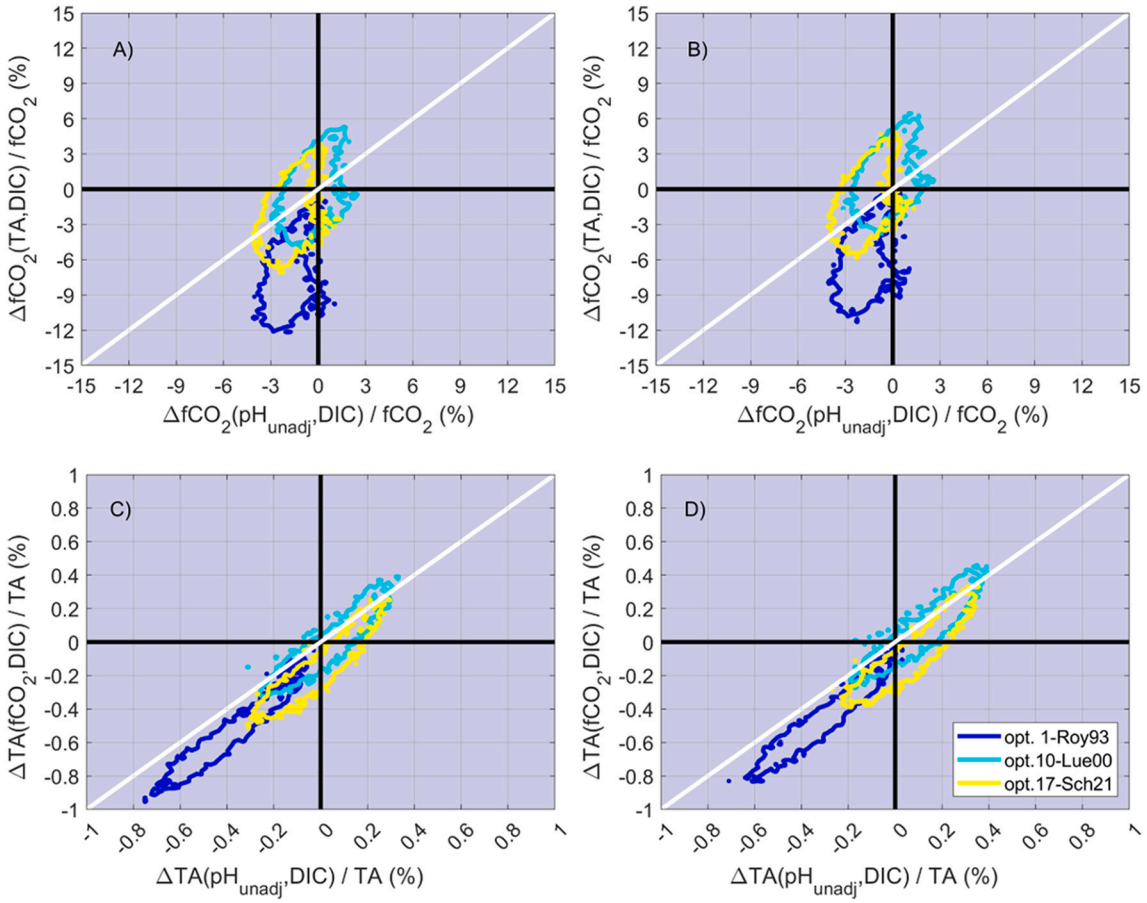

Fig. 5. Distribution of the isoline 1.1 of the two-dimensional histograms in Fig. 4 for (A-B) ΔfCO_2(TA,DIC)/fCO_2 versus ΔfCO_2(pH_{unadj},DIC)/fCO_2 (both in %); and (C-D) $\Delta TA(fCO_2,DIC)/TA$ versus $\Delta TA(pH_{unadj},DIC)/TA$ (both in %) resulting from using different carbonic acid dissociation constants and r_B. Navy (opt. 1-Roy93) represents the results using the carbonic acid dissociation constants of Roy et al. (1993), cyan (opt. 10-Lue00) using those of Mehrbach et al. (1973) refitted by Lueker et al. (2000), and yellow (opt. 17-Sch21) using the K_1 of Waters et al. (2014) and the K_1K_2 of Schockman and Byrne (2021). The isoline 1.1 envelopes the region where the number of samples per bin (0.3% for ΔfCO_2 and 0.02% for ΔTA) is $> 10^{1.1}$, i.e., > 13 samples per bin. Subplots (A) and (C) show the results when using the r_B of Lee et al. (2010), while (B) and (D) show the results when using the r_B of Uppström (1974). Note that the carbonic acid dissociation constants of Roy et al. (1993) were determined in artificial seawater, while the others were determined in natural seawater. Calculations were performed at sample salinity and atmospheric pressure. (For interpretation of the references to color in this figure legend, the reader is referred to the web version of this article.)

difference of 300 µatm between the fCO_2 of the sample and the gas standard would generate an uncertainty of about 1 µatm (Kevin Sullivan, pers. comm.). Therefore, the equilibration perturbation should be a minor contributor to the uncertainty of the measurements.

3.3. pH measurements

The negative ΔfCO_2(pH,DIC) values (Fig. 3A; recall, Δ, measured minus calculated variable) could be derived from an underestimation of measured pH (Fig. S2) resulting from (i) the non-use of the DelValls and Dickson (1998) correction, and/or (ii) the use of unpurified indicators for the pH measurements (Liu et al., 2011).

Cruise metadata did not state if the pH values in our dataset (Fig. 1; Table S1) were corrected according to DelValls and Dickson (1998) (i.e., increasing pH by 0.0047 units). Applying the DelValls and Dickson (1998)'s correction to our dataset will displace the ΔfCO_2 values by 1% towards positive values (Figs. S2A, and S8A), therefore worsening the internal consistency of the dataset.

All pH measurements included in this work were performed using unpurified indicators (Table S1). The use of unpurified indicators biases pH measurements towards lower values with respect to those performed with purified indicators, especially at high-pH values (Liu et al., 2011). As an approximation of the influence of indicator impurities in our internal consistency assessment, we applied an unpurified to purified pH correction as if all indicators were from the same manufacturer, either Acros (since it presented the highest discrepancies in Fig. 2A in Liu et al. (2011)) or TCl (since it presented the lowest discrepancies in Fig. 2A in Liu et al. (2011)). We corrected the pH values from our compiled dataset by subtracting the ΔpH observed by Liu et al. (2011) for each indicator. This rough correction into purified indicator pH values shifts the ΔfCO_2 towards positive values, reducing its internal consistency, especially at high-pH values and for indicators with a greater effect from impurities (changing ΔfCO_2(pH,DIC) from $-0.3 \pm 2\%$ to $2.5 \pm 2\%$ and $0.7 \pm 2\%$ for the Across and TCl approximations, respectively), and increasing the pH-dependency of ΔfCO_2 (Fig. S8B). This result points to indicator impurities not being the main source of the internal inconsistencies in our dataset.

3.4. DIC and TA measurements

The group of positive ΔfCO_2(TA,DIC) at low-pH values (pH ≈ 7.6; Fig. 3C) cannot be uniquely explained by the propagation of the standard uncertainty in the two input variables (4 µmol kg^{-1}) or by overestimating measured fCO_2, which is unlikely for high-fCO_2 values. The possible causes for the positive ΔfCO_2(TA,DIC) (recall, Δ, measured minus calculated variable) are (i) the underestimation of DIC linked to sample outgassing and/or (ii) the presence of OrgAlk in the samples (therefore, overestimating the sample TA).

Inter-laboratory comparison exercises yielded more uncertain DIC measurements for the high-CO_2 samples than for those with CO_2 levels closer to current atmospheric values (Bockmon and Dickson, 2015). Those results suggested a CO_2 loss during analysis yielding DIC underestimation proportional to the DIC of the sample. If we model a potential CO_2 loss by linearly increasing DIC proportionally to the sample DIC by up to 5 μmol kg^{-1}, ΔfCO_2(TA,DIC) is displaced towards negative values (from $-0.3 \pm 2\%$ to $-2.6 \pm 3\%$), thus worsening the internal consistency evidenced by the decrease in the percentage of data comprised within limits of uncertainty (from 88% to 72%) (Fig. S9A). However, hints for DIC underestimation are observed in some cruises where positive ΔfCO_2 values are present for fCO_2(TA,DIC) but not for fCO_2(pH, DIC) (or for fCO_2(pH,TA), results not shown) (scatter plots of the residuals by cruises are not shown; but these hints for DIC underestimation can be observed in Figs. S4, and S6A and C). Note that uncertainties or biases in DIC measurements play a bigger role in the uncertainty of fCO_2(TA,DIC) than in fCO_2(pH,DIC) (Figs. S2, and S3). Due to the small role that uncertainties in DIC play in fCO_2(pH,DIC), correcting DIC for the possible outgassing of up to 5 μmol kg^{-1} does not change the ΔfCO_2(pH,DIC) distributions (not shown).

The magnitude, distribution (Millero et al., 2002; Fong and Dickson, 2019; Álvarez et al., 2020), and detection (Song et al., 2020; Kerr et al., 2021) of OrgAlk in open ocean waters are controversial. Based on comparisons between measured and calculated TA, OrgAlk is estimated to be ~4–8 μmol kg^{-1} in open ocean waters (Millero et al., 2002; Fong and Dickson, 2019) but could be > 100 μmol kg^{-1} in estuarine waters (Cai et al., 1999). The discrepancy between measured and calculated TA is still to be solved by direct measurements of OrgAlk, which remains challenging (Kerr et al., 2021). Correcting the compiled dataset for a speculative excess in sample TA of 4 μmol kg^{-1} results in an increase of about 3% in calculated fCO_2 (Fig. S3A) and, consequently, the ΔfCO_2(TA,DIC) distribution is displaced towards negative values, reducing the internal consistency of the dataset (Fig. S9B). Therefore, OrgAlk is not he main source of the internal inconsistencies in our dataset.

If we assume a combination of the possible biases in TA (reduced in 4 μmol kg^{-1} due to a speculative excess of TA) and DIC (measured DIC proportionally increased up to 5 μmol kg^{-1} due to CO_2 outgassing) and correct the compiled dataset for both of them, then the ΔfCO_2(TA,DIC) distribution is displaced towards negative values outside the area of internal consistency (Fig. S9C).

3.5. Influence of the thermodynamic constants

Assuming an uncertainty of 4 μmol kg^{-1} in DIC and TA and 0.01 in pH, the uncertainty introduced in calculated fCO_2 is 2–4% (low to high pH waters) for fCO_2(TA,DIC) and 2.2–2.8% for fCO_2(pH,DIC) (Fig. 2). However, these uncertainties increase to 4–4.5% and 3–3.5%, respectively, when considering the uncertainties for pK_1 (0.0075), pK_2 (0.015), and the other thermodynamic constants (Orr et al., 2018) (Figs. 2, and 3). Besides, the effect introduced by uncertainties in the thermodynamic constants is larger for high-pH waters (Fig. 2). The interplay between the uncertainties in the input variables and thermodynamic constants (pK_1, pK_2, pK_B, and r_B) involved in calculating fCO_2(TA,DIC) makes the DIC-TA pair a less suitable option for estimating fCO_2 than the pH-DIC pair, even when high-quality measurements are used.

As discussed in previous works (e.g., Lee et al., 2010; Raimondi et al., 2019; Olafsson et al., 2020; Woosley, 2021), using carbonic acid dissociation constants determined in natural seawater generates the best internal consistency results (compare blue lines with cyan and yellow lines in Fig. 5). We note that the selection of the r_B plays a minor role in the residuals, with the use of the r_B of Uppström (1974) displacing the residuals towards positive values with respect to the use of the r_B of Lee et al. (2010) (compare left and right plots in Fig. 5), but with no clear gain or detriment to the internal consistency of our dataset. The $\Delta fCO_2/fCO_2$ resulting from using the constants derived by Lueker et al. (2000) yield the more internally consistent results highlighted by residuals centered around zero, as was already highlighted by Millero et al. (2002). The new K_1K_2 values of Schockman and Byrne (2021) displaces the $\Delta fCO_2/fCO_2$ distribution towards negative values compared to those from Lueker et al. (2000) (compare yellow and cyan lines in Fig. 5), worsening the internal consistency of our dataset.

When using DIC and TA as input variables, uncertainties in calculated fCO_2 mostly depend on uncertainties in pK_2. However, only a reliable pK_1 is needed when calculating fCO_2 from pH-DIC (or pH-TA). The better internal consistency between fCO_2, pH, and DIC compared to that between fCO_2, TA, and DIC (Fig. 3) suggests that the parameterization of pK_2 needs to be reformulated. However, the new K_1K_2 parameterizations of Schockman and Byrne (2021) do not improve the internal consistency of the measurements with respect to using the parameterizations of Lueker et al. (2000). The fact that updated K_2 values based on spectrophotometric pH determination using purified indicators do not improve the internal consistency of the seawater carbonate system suggests the need to refine the whole thermodynamic model of the seawater carbonate system using natural seawater and the methodologies used in the measurements of the seawater carbonate system.

On the other hand, it would be reasonable to suggest the reexamination of the K_0 parameterization (Lee et al., 1997; McElligott et al., 1998). However, the 0.6% offset observed by Lueker (1998) from the parameterization recommended by Weiss (1974) is not sufficiently large to cause the observed trend in ΔfCO_2 (Lueker, 1998). Besides, the influence of uncertainties in K_0 is minor in the internal consistency of the seawater carbonate system (Orr et al., 2018).

3.6. Conclusions and future perspectives

The agreement between measurements and thermodynamic calculations of the variables of the seawater carbonate system is fundamental to evaluating and understanding the current and future oceanic carbon sink and the chemical changes associated with ocean acidification. Autonomous measurements of water column pH (Bushinsky et al., 2019) and surface fCO_2 (Bakker et al., 2016) are becoming increasingly important to monitor the oceanic carbon cycle. Accordingly, pH and fCO_2 should be calculated with reduced uncertainty from TA and DIC, and vice versa, as many data-based studies (e.g., Lauvset et al., 2020) and global ocean biogeochemical models (e.g., Hauck et al., 2020; Mongin et al., 2021) on ocean pH and the oceanic carbon sink are derived from DIC and TA. Besides, uncertainties in the thermodynamic constants have a larger effect in surface waters (high-pH waters), where ocean acidification is to be monitored. Therefore, the reevaluation of the thermodynamic constants is necessary, especially K_2, which is of utmost need for the DIC and TA input pair.

Overall, the current internal consistency of the seawater carbonate system in the selected dataset is better than ± 3% for fCO_2 when pH is one of the input variables. Using the DIC-TA input pair, the internal consistency worsens to about 4% for calculated fCO_2. Therefore, if fCO_2 cannot be measured, we recommend calculating it from pH and DIC.

Our work highlights the good internal consistency between DIC, fCO_2, and pH measurements performed using unpurified indicators; therefore, discarding the indicator impurities as the main source of internal inconsistencies. However, using unpurified and purified indicators for pH measurements might create a mismatch in ocean acidification rates. Correcting pH measurements for indicator impurities will be challenging for the community since it requires the availability of the unpurified indicator used and the original absorbance data (Liu et al., 2011; Douglas and Byrne, 2017). The original unpurified indicator used may be unavailable for historical cruises, and the original absorbance data is not included in international databases, making it difficult or even impossible to correct historical pH measurements performed with unpurified indicators to agree with pH measurements performed with purified indicators. Besides, the lack of CRMs for pH also precludes improving the accuracy and precision of the measurements.

Since the creation of the SOPs for the seawater carbonate system measurements (Dickson et al., 2007), details on the methodologies have evolved, especially for pH (Ma et al., 2019; Álvarez et al., 2020). Therefore, to improve the precision and accuracy of the measurements of the seawater carbonate system, the SOPs need to be updated according to current technological and analytical advances. Besides, the production of CRMs for TA and DIC over the range of values encountered in the global ocean should be a priority, along with corresponding CRMs for fCO_2 and pH. High-CO_2 CRMs at laboratory temperature represent perhaps a major challenge both in their manufacturing phase and in their handling in the laboratory, but they would help to tackle the poorer internal consistencies for high-fCO_2 values. Besides, special attention should be devoted to understanding and quantifying the excess alkalinity ascribed to organic compounds. Last but not least, increasing the number of discrete water column fCO_2 measurements globally, which are even scarcer than pH measurements, would help to detect inconsistencies in the seawater carbonate system; and help to improve the intercomparability of the seawater carbonate system variables. We would also recommend that other laboratories use the fCO_2 methodology, so its applicability and results can be widely tested and validated.

Our study highlights the need to holistically reassess the seawater carbonate system as already proposed by McElligott et al. (1998) more than 20 years ago, and not partially as has been done to date. This reassessment of the seawater carbonate system as a whole will enable detecting changes at the climatic level of all the system variables, both from measurements and calculated variables, which is essential to detect changes in ocean chemistry related to CO_2 uptake and design potential ocean-based solutions to mitigate global change.

Author contributions

The manuscript was written through the contributions of all authors. All authors have approved the final version of the manuscript. M.I.G-I. and M.A. contributed equally to this work. All authors contributed to the interpretation of the data and the discussion of the results presented in the manuscript.

Funding

The research leading to these results was supported through NOAA's Ocean Acidification Program (OAP) via Award #NA17OAR0170332; through NERC via project NE/P021263/1; through the Spanish Research Agency via project PID2019-104279GB-C21/AEI/10.13039/501100011033; and through GAIN via grant IN607A2018/2.

Declaration of Competing Interest

None.

Data availability

The data is publicly available in GLODAP (https://www.glodap.info/).

Acknowledgments

We are grateful to the captains, staff, and researchers who contributed to acquiring and processing the hydrographic data. For this work, M.I. García-Ibáñez was supported by NOAA's Ocean Acidification Program (OAP) via Award #NA17OAR0170332, and by NERC's CUSTARD (Carbon Uptake and Seasonal Traits of Antarctic Remineralisation Depths) project NE/P021263/1. N.M. Fajar was supported by grant IN607A2018/2 from the Axencia Galega de Innovación (GAIN, Xunta de Galicia, Spain). F.F. Pérez was supported by the BOCATS2 (PID2019-104279GB-C21) project funded by MCIN/AEI/10.13039/501100011033 and contributed to WATER:iOS CSIC PTI. W.-J. Cai was supported by NOAA's Ocean Acidification Program (OAP) via Award #NA17OAR0170332. M. Álvarez was supported by the RADPROF project. This work acknowledges the 'Severo Ochoa Centre of Excellence' accreditation (CEX2019-000928-S). We are grateful to the Ocean Carbon Biogeochemistry program for funding the Ocean Carbonate System Intercomparison Forum (OCSIF) working group, which helped foster this work. We thank the three anonymous reviewers whose insightful comments and suggestions helped improve and clarify this manuscript.

Appendix A. Supplementary data

Supplementary data to this article can be found online at https://doi.org/10.1016/j.marchem.2022.104150.

References

Álvarez, M., Fajar, N.M., Carter, B.R., Guallart, E.F., Pérez, F.F., Woosley, R.J., Murata, A., 2020. Global ocean spectrophotometric pH assessment: consistent inconsistencies. Environ. Sci. Technol. 54, 10977–10988. https://doi.org/10.1021/acs.est.9b06932.

Bakker, D.C.E., Pfeil, B., Landa, C.S., Metzl, N., O'Brien, K.M., Olsen, A., Smith, K., Cosca, C., Harasawa, S., Jones, S.D., Nakaoka, S., Nojiri, Y., Schuster, U., Steinhoff, T., Sweeney, C., Takahashi, T., Tilbrook, B., Wada, C., Wanninkhof, R., Alin, S.R., Balestrini, C.F., Barbero, L., Bates, N.R., Bianchi, A.A., Bonou, F., Boutin, J., Bozec, Y., Burger, E.F., Cai, W.-J., Castle, R.D., Chen, L., Chierici, M., Currie, K., Evans, W., Featherstone, C., Feely, R.A., Fransson, A., Goyet, C., Greenwood, N., Gregor, L., Hankin, S., Hardman-Mountford, N.J., Harlay, J., Hauck, J., Hoppema, M., Humphreys, M.P., Hunt, C.W., Huss, B., Ibánhez, J.S.P., Johannessen, T., Keeling, R., Kitidis, V., Körtzinger, A., Kozyr, A., Krasakopoulou, E., Kuwata, A., Landschützer, P., Lauvset, S.K., Lefèvre, N., Lo Monaco, C., Manke, A., Mathis, J.T., Merlivat, L., Millero, F.J., Monteiro, P.M.S., Munro, D.R., Murata, A., Newberger, T., Omar, A.M., Ono, T., Paterson, K., Pearce, D., Pierrot, D., Robbins, L. L., Saito, S., Salisbury, J., Schlitzer, R., Schneider, B., Schweitzer, R., Sieger, R., Skjelvan, I., Sullivan, K.F., Sutherland, S.C., Sutton, A.J., Tadokoro, K., Telszewski, M., Tuma, M., van Heuven, S.M.A.C., Vandemark, D., Ward, B., Watson, A.J., Xu, S., 2016. A multi-decade record of high-quality fCO_2 data in version 3 of the Surface Ocean CO_2 atlas (SOCAT). Earth Syst. Sci. Data 8, 383–413. https://doi.org/10.5194/essd-8-383-2016.

Bittig, H.C., Steinhoff, T., Claustre, H., Fiedler, B., Williams, N.L., Sauzède, R., Körtzinger, A., Gattuso, J.-P., 2018. An alternative to static climatologies: robust estimation of open ocean CO2 variables and nutrient concentrations from T, S, and O2 data using Bayesian neural networks. Front. Mar. Sci. 5, 328. https://doi.org/10.3389/fmars.2018.00328.

Bockmon, E.E., Dickson, A.G., 2015. An inter-laboratory comparison assessing the quality of seawater carbon dioxide measurements. Mar. Chem. 171, 36–43. https://doi.org/10.1016/j.marchem.2015.02.002.

Bushinsky, S.M., Takeshita, Y., Williams, N.L., 2019. Observing changes in ocean carbonate chemistry: our autonomous future. Curr. Clim. Change Rep. 5, 207–220. https://doi.org/10.1007/s40641-019-00129-8.

Cai, W.-J., Pomeroy, L.R., Moran, M.A., Wang, Y., 1999. Oxygen and carbon dioxide mass balance for the estuarine-intertidal marsh complex of five rivers in the southeastern U.S. Limnol. Oceanogr. 44, 639–649. https://doi.org/10.4319/lo.1999.44.3.0639.

Caldeira, K., Wickett, M.E., 2003. Oceanography: anthropogenic carbon and ocean pH. Nature 425, 365. https://doi.org/10.1038/425365a.

Chen, H., Wanninkhof, R., Feely, R.A., Greeley, D., 1995. Measurement of Fugacity of Carbon Dioxide in Subsurface Water: An Evaluation of a Method Based on Infrared Analysis (No. ERL AOML-85). NOAA Technical Report.

Clayton, T.D., Byrne, R.H., 1993. Spectrophotometric seawater pH measurements: total hydrogen ion concentration scale calibration of m-cresol purple and at-sea results. Deep-Sea Res. I Oceanogr. Res. Pap. 40, 2115–2129. https://doi.org/10.1016/0967-0637(93)90048-8.

DelValls, T., Dickson, A., 1998. The pH of buffers based on 2-amino-2-hydroxymethyl-1, 3-propanediol ('tris') in synthetic sea water. Deep-Sea Res. I 45, 1541–1554. https://doi.org/10.1016/s0967-0637(98)00019-3.

Dickson, A., 2010. Standards for Ocean Measurements, 23. Oceanog., pp. 34–47. https://doi.org/10.5670/oceanog.2010.22

Dickson, A.G., 1990. Standard potential of the reaction: $AgCl(s) + 12H_2(g) = Ag(s) + HCl(aq)$, and the standard acidity constant of the ion HSO_4^- in synthetic sea water from 273.15 to 318.15 K. J. Chem. Thermodyn. 22, 113–127.

Dickson, A.G., Sabine, C.L., Christian, J.R., 2007. Guide to Best Practices for Ocean CO_2 Measurements. North Pacific Marine Science Organization Sidney, British Columbia.

Douglas, N.K., Byrne, R.H., 2017. Achieving accurate spectrophotometric pH measurements using unpurified meta-cresol purple. Mar. Chem. 190, 66–72. https://doi.org/10.1016/j.marchem.2017.02.004.

Fong, M.B., Dickson, A.G., 2019. Insights from GO-SHIP hydrography data into the thermodynamic consistency of CO2 system measurements in seawater. Mar. Chem. 211, 52–63. https://doi.org/10.1016/j.marchem.2019.03.006.

Friedlingstein, P., Jones, M.W., O'Sullivan, M., Andrew, R.M., Bakker, D.C.E., Hauck, J., Le Quéré, C., Peters, G.P., Peters, W., Pongratz, J., Sitch, S., Canadell, J.G., Ciais, P.,

Jackson, R.B., Alin, S.R., Anthoni, P., Bates, N.R., Becker, M., Bellouin, N., Bopp, L., Chau, T.T.T., Chevallier, F., Chini, L.P., Cronin, M., Currie, K.I., Decharme, B., Djeutchouang, L.M., Dou, X., Evans, W., Feely, R.A., Feng, L., Gasser, T., Gilfillan, D., Gkritzalis, T., Grassi, G., Gregor, L., Gruber, N., Gürses, Ö., Harris, I., Houghton, R. A., Hurtt, G.C., Iida, Y., Ilyina, T., Luijkx, I.T., Jain, A., Jones, S.D., Kato, E., Kennedy, D., Klein Goldewijk, K., Knauer, J., Korsbakken, J.I., Körtzinger, A., Landschützer, P., Lauvset, S.K., Lefèvre, N., Lienert, S., Liu, J., Marland, G., McGuire, P.C., Melton, J.R., Munro, D.R., Nabel, J.E.M.S., Nakaoka, S.-I., Niwa, Y., Ono, T., Pierrot, D., Poulter, B., Rehder, G., Resplandy, L., Robertson, E., Rödenbeck, C., Rosan, T.M., Schwinger, J., Schwingshackl, C., Séférian, R., Sutton, A.J., Sweeney, C., Tanhua, T., Tans, P.P., Tian, H., Tilbrook, B., Tubiello, F., van der Werf, G.R., Vuichard, N., Wada, C., Wanninkhof, R., Watson, A.J., Willis, D., Wiltshire, A.J., Yuan, W., Yue, C., Yue, X., Zaehle, S., Zeng, J., 2022. Global Carbon Budget 2021. Earth Syst. Sci. Data 14, 1917–2005. https://doi.org/10.5194/essd-14-1917-2022.

Gattuso, J.-P., Brewer, P.G., Hoegh-Guldberg, O., Kleypas, J.A., Pörtner, H.-O., Schmidt, D.N., Field, C.B., Barros, V.R., Dokken, D.J., Mach, K.J., Mastrandrea, M.D., Bilir, T.E., Chatterjee, M., Ebi, K.L., Estrada, Y.O., Genova, R.C., Girma, B., Kissel, E. S., Levy, A.N., Maccracken, S., Mastrandrea, P.R., White, L.L., 2014. Cross-chapter box on ocean acidification. In: IPCC, 2014: Climate Change 2014: Impacts, Adaptation, and Vulnerability. Part A: Global and Sectoral Aspects. Contribution of Working Group II to the Fifth Assessment Report of the Intergovernmental Panel on Climate Change. Cambridge University Press, Cambridge, United Kingdom and New York, NY, USA, pp. 129–131.

Gruber, N., Clement, D., Carter, B.R., Feely, R.A., van Heuven, S., Hoppema, M., Ishii, M., Key, R.M., Kozyr, A., Lauvset, S.K., Monaco, C.L., Mathis, J.T., Murata, A., Olsen, A., Perez, F.F., Sabine, C.L., Tanhua, T., Wanninkhof, R., 2019. The oceanic sink for anthropogenic CO2 from 1994 to 2007. Science 363, 1193–1199. https://doi.org/10.1126/science.aau5153.

Guidi, L., Fernàndez-Guerra, A., Canchaya, C., Curry, E., Foglini, F., Irission, J.-O., Malde, K., Marshall, C.T., Obst, M., Ribeiro, R.P., Tjiputra, J., Bakker, D.C.E., 2020. Big data in marine science, in: future science brief 6 of the European marine B. Zenodo. https://doi.org/10.5281/zenodo.3755793.

Hauck, J., Zeising, M., Le Quéré, C., Gruber, N., Bakker, D.C.E., Bopp, L., Chau, T.T.T., Gürses, Ö., Ilyina, T., Landschützer, P., Lenton, A., Resplandy, L., Rödenbeck, C., Schwinger, J., Séférian, R., 2020. Consistency and challenges in the ocean carbon sink estimate for the global carbon budget. Front. Mar. Sci. 7, 852. https://doi.org/10.3389/fmars.2020.571720.

Kerr, D.E., Brown, P.J., Grey, A., Kelleher, B.P., 2021. The influence of organic alkalinity on the carbonate system in coastal waters. Mar. Chem. 237, 104050 https://doi.org/10.1016/j.marchem.2021.104050.

Lauvset, S.K., Carter, B.R., Pérez, F.F., Jiang, L.-Q., Feely, R.A., Velo, A., Olsen, A., 2020. Processes driving global Interior Ocean pH distribution. Glob. Biogeochem. Cycles 34. https://doi.org/10.1029/2019GB006229.

Lauvset, S.K., Lange, N., Tanhua, T., Bittig, H.C., Olsen, A., Kozyr, A., Álvarez, M., Becker, S., Brown, P.J., Carter, B.R., Cotrim da Cunha, L., Feely, R.A., van Heuven, S., Hoppema, M., Ishii, M., Jeansson, E., Jutterström, S., Jones, S.D., Karlsen, M.K., Lo Monaco, C., Michaelis, P., Murata, A., Pérez, F.F., Pfeil, B., Schirnick, C., Steinfeldt, R., Suzuki, T., Tilbrook, B., Velo, A., Wanninkhof, R., Woosley, R.J., Key, R.M., 2021. An updated version of the global interior ocean biogeochemical data product, GLODAPv2.2021. Earth Syst. Sci. Data 13, 5565–5589. https://doi.org/10.5194/essd-13-5565-2021.

Lee, K., Millero, F.J., Wanninkhof, R., 1997. The carbon dioxide system in the Atlantic Ocean. J. Geophys. Res. 102, 15693–15.

Lee, K., Kim, T.-W., Byrne, R.H., Millero, F.J., Feely, R.A., Liu, Y.-M., 2010. The universal ratio of boron to chlorinity for the North Pacific and North Atlantic oceans. Geochim. Cosmochim. Acta 74, 1801–1811. https://doi.org/10.1016/j.gca.2009.12.027.

Liu, X., Patsavas, M.C., Byrne, R.H., 2011. Purification and characterization of meta-cresol purple for spectrophotometric seawater pH measurements. Environ. Sci. Technol. 45, 4862–4868. https://doi.org/10.1021/es200665d.

Lueker, T.J., 1998. Carbonic Acid Dissociation Constants Determined as the Ratio K1/K2 from the Concentration of CO2 in Gas and Seawater Equilibrium. University of California San Diego.

Lueker, T.J., Dickson, A.G., Keeling, C.D., 2000. Ocean pCO2 calculated from dissolved inorganic carbon, alkalinity, and equations for K1 and K2: validation based on laboratory measurements of CO2 in gas and seawater at equilibrium. Mar. Chem. 70, 105–119. https://doi.org/10.1016/S0304-4203(00)00022-0.

Ma, J., Shu, H., Yang, B., Byrne, R.H., Yuan, D., 2019. Spectrophotometric determination of pH and carbonate ion concentrations in seawater: choices, constraints and consequences. Anal. Chim. Acta 1081, 18–31. https://doi.org/10.1016/j.aca.2019.06.024.

McElligott, S., Byrne, R.H., Lee, K., Wanninkhof, R., Millero, F.J., Feely, R.A., 1998. Discrete water column measurements of CO2 fugacity and pHT in seawater: a comparison of direct measurements and thermodynamic calculations. Mar. Chem. 60, 63–73. https://doi.org/10.1016/S0304-4203(97)00080-7.

Mehrbach, C., Culberson, C.H., Hawley, J.E., Pytkowicz, R.M., 1973. Measurement of the apparent dissociation constants of carbonic acid in seawater at atmospheric pressure. Limnol. Oceanogr. 18, 897–907. https://doi.org/10.4319/lo.1973.18.6.0897.

Millero, F.J., 2007. The marine inorganic carbon cycle. Chem. Rev. 107, 308–341. https://doi.org/10.1021/cr0503557.

Millero, F.J., Pierrot, D., Lee, K., Wanninkhof, R., Feely, R., Sabine, C.L., Key, R.M., Takahashi, T., 2002. Dissociation constants for carbonic acid determined from field measurements. Deep-Sea Res. I Oceanogr. Res. Pap. 49, 1705–1723.

Mongin, M., Baird, M.E., Lenton, A., Neill, C., Akl, J., 2021. Reversing Ocean Acidification along the Great Barrier Reef Using Alkalinity Injection.

Neill, C., Johnson, K.M., Lewis, E., Wallace, D.W., 1997. Accurate headspace analysis of fCO2 in discrete water samples using batch equilibration. Limnol. Oceanogr. 42, 1774–1783.

Newton, J., Feely, R., Jewett, E., Williamson, P., Mathis, J., 2015. Global Ocean Acidification Observing Network: Requirements and Governance Plan.

Olafsson, J., Lee, K., Olafsdottir, S.R., Benoit-Cattin, A., Lee, C.-H., Kim, M., 2020. Boron to salinity ratios for Atlantic, Arctic and polar Waters: a view from downstream. Mar. Chem. 224, 103809 https://doi.org/10.1016/j.marchem.2020.103809.

Olsen, A., Lange, N., Key, R.M., Tanhua, T., Álvarez, M., Becker, S., Bittig, H.C., Carter, B. R., Cotrim da Cunha, L., Feely, R.A., van Heuven, S., Hoppema, M., Ishii, M., Jeansson, E., Jones, S.D., Jutterström, S., Karlsen, M.K., Kozyr, A., Lauvset, S.K., Monaco, C.L., Murata, A., Pérez, F.F., Pfeil, B., Schirnick, C., Steinfeldt, R., Suzuki, T., Telszewski, M., Tilbrook, B., Velo, A., Wanninkhof, R., 2019. GLODAPv2.2019 – an update of GLODAPv2. Earth Syst. Sci. Data 11, 1437–1461. https://doi.org/10.5194/essd-11-1437-2019.

Olsen, A., Lange, N., Key, R.M., Tanhua, T., Bittig, H.C., Kozyr, A., Álvarez, M., Azetsu-Scott, K., Becker, S., Brown, P.J., Carter, B.R., Cotrim da Cunha, L., Feely, R.A., van Heuven, S., Hoppema, M., Ishii, M., Jeansson, E., Jutterström, S., Landa, C.S., Lauvset, S.K., Michaelis, P., Murata, A., Pérez, F.F., Pfeil, B., Schirnick, C., Steinfeldt, R., Suzuki, T., Tilbrook, B., Velo, A., Wanninkhof, R., Woosley, R.J., 2020. An updated version of the global interior ocean biogeochemical data product, GLODAPv2.2020. Earth Syst. Sci. Data 12, 3653–3678. https://doi.org/10.5194/essd-12-3653-2020.

Orr, J.C., Epitalon, J.-M., Dickson, A.G., Gattuso, J.-P., 2018. Routine uncertainty propagation for the marine carbon dioxide system. Mar. Chem. 207, 84–107. https://doi.org/10.1016/j.marchem.2018.10.006.

Park, P.K., 1969. Oceanic Co2 system: an evaluation of ten methods of Investigation1. Limnol. Oceanogr. 14, 179–186. https://doi.org/10.4319/lo.1969.14.2.0179.

Raimondi, L., Matthews, J.B.R., Atamanchuck, D., Azetsu-Scott, K., Wallace, D., 2019. The internal consistency of the marine carbon dioxide system for high latitude shipboard and in situ monitoring. Mar. Chem. 213, 49–70. https://doi.org/10.1016/j.marchem.2019.03.001.

Raven, J., Caldeira, K., Elderfield, H., Hoegh-Guldberg, O., Liss, P., Riebesell, U., Shepherd, J., Turley, C., Watson, A., 2005. Ocean Acidification Due to Increasing Atmospheric Carbon Dioxide. The Royal Society, London. Document No. 12/05.

Ribas-Ribas, M., Rérolle, V.M.C., Bakker, D.C.E., Kitidis, V., Lee, G.A., Brown, I., Achterberg, E.P., Hardman-Mountford, N.J., Tyrrell, T., 2014. Intercomparison of carbonate chemistry measurements on a cruise in northwestern European shelf seas. Biogeosciences 11, 4339–4355. https://doi.org/10.5194/bg-11-4339-2014.

Roy, R.N., Roy, L.N., Vogel, K.M., Porter-Moore, C., Pearson, T., Good, C.E., Millero, F.J., Campbell, D.M., 1993. The dissociation constants of carbonic acid in seawater at salinities 5 to 45 and temperatures 0 to 45°C. Mar. Chem. 44, 249–267.

Sabine, C., Key, R., Kozyr, A., Feely, R., Wanninkhof, R., Millero, F., Peng, T., Bullister, J., Lee, K., 2005. Global Ocean Data Analysis Project (GLODAP): Results and Data, NDP-083, p. 110 (Carbon Dioxide Inf. Anal. Cent., Oak Ridge Natl. Lab., Oak Ridge, Tenn).

Schockman, K.M., Byrne, R.H., 2021. Spectrophotometric determination of the bicarbonate dissociation constant in seawater. Geochim. Cosmochim. Acta. https://doi.org/10.1016/j.gca.2021.02.008.

Sharp, J.D., Pierrot, D., Humphreys, M.P., Epitalon, J.-M., Orr, J.C., Lewis, E.R., Wallace, D.W.R., 2020. CO2SYSv3 for MATLAB. Zenodo. https://doi.org/10.5281/zenodo.3952803.

Song, S., Wang, Z.A., Gonneea, M.E., Kroeger, K.D., Chu, S.N., Li, D., Liang, H., 2020. An important biogeochemical link between organic and inorganic carbon cycling: effects of organic alkalinity on carbonate chemistry in coastal waters influenced by intertidal salt marshes. Geochim. Cosmochim. Acta 275, 123–139. https://doi.org/10.1016/j.gca.2020.02.013.

Sulpis, O., Lauvset, S.K., Hagens, M., 2020. Current estimates of K_1* and K_2* appear inconsistent with measured CO_2 system parameters in cold oceanic regions. Ocean Sci. 16, 847–862. https://doi.org/10.5194/os-16-847-2020.

Takeshita, Y., Johnson, K.S., Martz, T.R., Plant, J.N., Sarmiento, J.L., 2018. Assessment of autonomous pH measurements for determining surface seawater partial pressure of CO2. J. Geophys. Res. Oceans 123, 4003–4013. https://doi.org/10.1029/2017JC013387.

Takeshita, Y., Warren, J.K., Liu, X., Spaulding, R.S., Byrne, R.H., Carter, B.R., DeGrandpre, M.D., Murata, A., Watanabe, S., 2021. Consistency and stability of purified meta-cresol purple for spectrophotometric pH measurements in seawater. Mar. Chem. 236, 104018 https://doi.org/10.1016/j.marchem.2021.104018.

Tanhua, T., Lauvset, S.K., Lange, N., Olsen, A., Álvarez, M., Diggs, S., Bittig, H.C., Brown, P.J., Carter, B.R., da Cunha, L.C., Feely, R.A., Hoppema, M., Ishii, M., Jeansson, E., Kozyr, A., Murata, A., Pérez, F.F., Pfeil, B., Schirnick, C., Steinfeldt, R., Telszewski, M., Tilbrook, B., Velo, A., Wanninkhof, R., Burger, E., O'Brien, K., Key, R.M., 2021. A vision for FAIR Ocean data products. Commun. Earth Environ. 2, 1–4. https://doi.org/10.1038/s43247-021-00209-4.

Uppström, L.R., 1974. The boron/chlorinity ratio of deep-sea water from the Pacific Ocean. Deep-Sea Res. Oceanogr. Abstr. 21, 161–162.

Wanninkhof, R., Thoning, K., 1993. Measurement of fugacity of CO2 in surface water using continuous and discrete sampling methods. In: Marine Chemistry, Marine Physical Chemistry - in memory of the contributions made to the field by Dr. Ricaerdo Pytkowicz, 44, pp. 189–204. https://doi.org/10.1016/0304-4203(93)90202-Y.

Wanninkhof, R., Tsung-Hung, P., Huss, B., Sabine, C.L., Lee, K., 2003. Comparison of inorganic carbon system parameters measured in the Atlantic Ocean from 1990 to 1998 and recommended adjustments. ORNL/CDIAC 140. https://doi.org/10.2172/814517.

Wanninkhof, R., Park, G.-H., Takahashi, T., Sweeney, C., Feely, R., Nojiri, Y., Gruber, N., Doney, S.C., McKinley, G.A., Lenton, A., Le Quéré, C., Heinze, C., Schwinger, J., Graven, H., Khatiwala, S., 2013a. Global Ocean carbon uptake: magnitude, variability and trends. Biogeosciences 10, 1983–2000. https://doi.org/10.5194/bg-10-1983-2013.

Wanninkhof, Rik, Park, G.-H., Takahashi, T., Feely, R.A., Bullister, J.L., Doney, S.C., 2013c. Changes in deep-water CO2 concentrations over the last several decades determined from discrete pCO2measurements. Deep-Sea Res. I Oceanogr. Res. Pap. 74, 48–63. https://doi.org/10.1016/j.dsr.2012.12.005.

Waters, J., Millero, F.J., Woosley, R.J., 2014. Corrigendum to "the free proton concentration scale for seawater pH", [MARCHE: 149 (2013) 8–22]. Mar. Chem. 165, 66–67. https://doi.org/10.1016/j.marchem.2014.07.004.

Weiss, R.F., 1974. Carbon dioxide in water and seawater: the solubility of a non-ideal gas. Mar. Chem. 2, 203–215. https://doi.org/10.1016/0304-4203(74)90015-2.

Williams, N.L., Juranek, L.W., Feely, R.A., Johnson, K.S., Sarmiento, J.L., Talley, L.D., Dickson, A.G., Gray, A.R., Wanninkhof, R., Russell, J.L., Riser, S.C., Takeshita, Y., 2017. Calculating surface ocean pCO2 from biogeochemical Argo floats equipped with pH: an uncertainty analysis. Glob. Biogeochem. Cycles 31, 591–604. https://doi.org/10.1002/2016GB005541.

Williamson, P., Widdicombe, S., 2018. The rise of CO2 and ocean acidification. In: Encyclopedia of the Anthropocene. Elsevier, New York City, pp. 51–59.

Woosley, R.J., 2021. Evaluation of the temperature dependence of dissociation constants for the marine carbon system using pH and certified reference materials. Mar. Chem. 229, 103914 https://doi.org/10.1016/j.marchem.2020.103914.